AFRL-VS-TR-2003-1551

IRRADIANCE CALIBRATION OF SPACE-BASED INFRARED SENSORS

Russell Walker
Martin Cohen

Monterey Institute for Research in Astronomy
200 Eighth Street
Marina, CA 93933

July 2002

Scientific Report No. 4

AIR FORCE RESEARCH LABORATORY
Space Vehicles Directorate
29 Randolph Rd
AIR FORCE MATERIEL COMMAND
HANSCOM AFB, MA 01731-3010

20031126 109

This technical report has been reviewed and is approved for publication.

/Signed/
TAMALYN BECKER, 2ND Lt, USAF
Contract Manager

/Signed/
ROBERT BELAND
Branch Chief

REPORT DOCUMENTATION PAGE

Form Approved
OMB No. 0704-0188

Public reporting burden for this collection of information is estimated to average 1 hour per response, including the time for reviewing instructions, searching existing data sources, gathering and maintaining the data needed, and completing and reviewing the collection of information. Send comments regarding this burden estimate or any other aspect of this collection of information, including suggestions for reducing this burden, to Washington Headquarters Services, Directorate for Information Operations and Reports, 1215 Jefferson Davis Highway, Suite 1204, Arlington, VA 22202-4302, and to the Office of Management and Budget, Paperwork Reduction Project (0704-0188), Washington, DC 20503.

1. AGENCY USE ONLY *(Leave blank)*	2. REPORT DATE July, 2002	3. REPORT TYPE AND DATES COVERED Annual Interim Report June 1, 2001 – May 31, 2002

4. TITLE AND SUBTITLE Irradiance Calibration of Space-Based Infrared Sensors, Scientific Report No. 4	5. FUNDING NUMBERS C F19628-98-C-0047 PR-MSX8 TA-BS WV-AE

6. AUTHORS Russell G. Walker and Martin Cohen	

7. PERFORMING ORGANIZATION NAME(S) AND ADDRESS(ES) Monterey Institute for Research in Astronomy 200 Eighth Street Marina, CA 93933	8. PERFORMING ORGANIZATION REPORT NUMBER VRISV-1130-AR03

9. SPONSORING/MONITORING AGENCY NAME(S) AND ADDRESS(ES) Air Force Research Laboratory/VSBYH 20 Randolph Road Hanscom AFB, MA 01731-3010	10. SPONSORING/MONITORING AGENCY REPORT NUMBER AFRL-VS-TR-2003-1551

11. SUPPLEMENTARY NOTES

12a. DISTRIBUTION/AVAILABILITY STATEMENT Approved for Public Release; Distribution Unlimited.	12b. DISTRIBUTION CODE

13. ABSTRACT *(Maximum 200 words)*
Abstract

The purpose of this work is to develop a basis for irradiance calibration of space-based infrared sensors. It is an extension of previous work that fully defines the context of the calibration, and the concepts of spectral composites and templates. We discuss four areas of work carried out during the past year; our accomplishments and failures; and our plans for the future. The four areas are:
1) Production and release of Version 4.0 of the Walker-Cohen Atlas of Calibrated Spectra,
2) Progress on the production of Version 2.0 of the Air Force Bright Spectral Atlas,
3) Exploration of the non-rejected Lunar radiance (NRLR) using the radiance data from the MSX Lunar OAR experiment DC32, and
4) Work on understanding the non-rejected Earth radiance that contaminated MSX CB01 scans of the zodiacal dust near the Sun.

14. SUBJECT TERMS Infrared, Calibration, Stars, Spectra, Off-axis radiance	15. NUMBER OF PAGES 25
	16. PRICE CODE

17. SECURITY CLASSIFICATION OF REPORT UNCLASSIFIED	18. SECURITY CLASSIFICATION OF THIS PAGE UNCLASSIFIED	19. SECURITY CLASSIFICATION OF ABSTRACT UNCLASSIFIED	20. LIMITATION OF ABSTRACT UL

NSN 7540-01-280-5500
(Rev 2-89)

Computer Generated

STANDARD FORM 298
Prescribed by ANSI Std 239-298-102

Contents

Figures

Tables

1. INTRODUCTION

Satellites employing infrared sensors are continually being launched by space agencies, such as NASA and ESA and by the US DoD community. The successes of IRAS, ISO, IRTS, and MSX have already produced enormous infrared databases. Consequently, there must now be greater emphasis on data verification, validation, and calibration issues to assure that these data sets are of sufficient reliability for application to the quantitative design of advanced space-borne sensors and systems. There is an urgent need not only to rationalize infrared calibration and place it in a common and well-defined context, but also to provide a network of calibrators well distributed across the sky, with a common traceable pedigree. This network should be sufficiently populated to have a member relatively close to any arbitrary direction because satellites and aircraft cannot afford major excursions in pointing to secure measurements of the few traditional calibration objects. Dynamic range, too, is an issue and such a network must include stars both fainter and brighter than today's popular "standards."

The purpose of this work is to develop a basis for irradiance calibration of space-based infrared sensors. It is an extension of previous work (Cohen, et al Papers I-IX, 1992-1998) that fully defines the context of the calibration, and the concepts of spectral composites and templates. This previous work culminated in the publication of *An All Sky Network of 422 Infrared Calibration Stars* (Cohen, et al 1999). Our approach is based on a self-consistent absolute framework within which radiometry and spectroscopy are unified, with wavelength coverage ideal for calibrating many satellite, airborne, and ground-based sensors.

Our work during the past year has been directed toward the following:

a) Production and release of Version 4 of the Walker-Cohen Atlas of Calibrated Spectra. Version 3 was an expansion of the original *All Sky Network of 422 Infrared Calibration Stars* to 570 stars using the results of the MSX observations and templates for additional spectral types. Version 4 now extends Version 3 to 617 stars by including some fainter stars, stars with revised spectral types, and new photometry archives.

b) Progress on the production of Version 2 of the Air Force Bright Spectral Atlas, which will include all of the stars from Version 1.1 plus additional stars that can now be fit with our more sophisticated grid of dusty model stellar atmospheres. The main thrust here is a more realistic representation of spectrum variability.

c) Exploration of the non-rejected Lunar radiance (NRLR) using the radiance data from the MSX Lunar OAR experiment DC32.

d) Work on understanding the non-rejected Earth radiance that contaminated MSX CB01 scans of the zodiacal dust near the Sun.

2. VERSION 4 OF THE WALKER-COHEN ATLAS OF CALIBRATED SPECTRA

The 603 templates issued under Release 4.0 were formulated following essentially the same principles as in previous releases. However, to make sure that templates (1.2-35 micron spectra) and our new "supertemplates" (0.11-35 micron templates) to be constructed for use by SIRTF's instruments are not represented by different spectral energy distributions where they overlap, several changes were made to the template code at this time. Appendix A, "Walker-Cohen Atlas Of Calibrated Spectra - Explanatory Supplement" describes these changes and their implementation in Release 4.0.

Much of the text in Appendix A duplicates the documentation accompanying Release 3.0 and has been retained for completeness between the published Release 2.1, and the new Release

4.0 network of stellar calibrators. However, wherever further changes have occurred between Releases 3.0 and 4.0, these are described in the appropriate sections.

The 617 spectra of Release 4 consist of 603 new templates, 3 models, and 11 composites. There are now 78 spectra for IRAS PSC-2 stars brighter than zero magnitude at 12 µm.

2.1 New Stars Templated

We have included 46 stars of the ISO "Ground-Based Preparatory Programme" had been represented for ISO purposes by Kurucz models. All these Kurucz "calibration spectra" lacked the SiO fundamental and were based on outdated CO line strengths. These stars are included in Release 4.0 and often are significantly fainter than the IRAS 12-micron flux density limit of 5 Jy that characterized our earlier releases.

We re-examined the stars used for calibration for the Mid-Infrared Spectrometer (MIRS) on the joint NASA-ISAS "Infrared Telescope in Space" mission. This yielded 19 new MIRS calibration stars, which have been included in the Release 4 templates.

We have further exercised COBE/DIRBE's own calibration network using the BCC archive (Mitchell et al., 1996), with the result that the templates for the latest type BCC calibrators are now improved in Release 4.0.

2.2 Revision of Extinction Corrections

Since Release 3.0 we have re-evaluated the intrinsic B-V color tables for K- and M-giants on the basis of substantial samples of these stars that were observed by Hipparcos. This, of course, led to re-evaluation of the extinction for any given star. In previous releases we chose to set the extinction to zero for those stars in which the application of the reddening ($Av<=0.044$) would result in less than a 1 percent change in the monochromatic flux density at a wavelength of 1 micron. However, in Release 4.0 we always applied the reddening regardless of the size of its effect in the near-infrared to avoid potential discrepancies between templates created by our conventional (1.2-35 micron) technique and supertemplates (0.11-35 micron spectra) created for SIRTF and other missions.

Zero extinction was found for 396 of the 603 template stars; the remaining 207 stars have extinctions between 0.02 and 1.77 magnitudes, with only 33 values exceeding 0.50 magnitudes.

3. VERSION 2 OF THE AIR FORCE BRIGHT SPECTRAL ATLAS

We have pursued two main areas directed toward the production of the AFBSA Version 2.0. The first has been to further develop and expand our photometric databases, and the second is to increase our library of infrared spectra through the addition of models of AGB stars.

3.1 Photometric Database

The irradiance levels of the spectra presented in AFBSA Versions 1.0 and 1.1 were determined by normalization of the IRAS Low Resolution Spectra (LRS) to the IRAS 12 µm inband irradiance. Spectra thus produced were subject to the full uncertainty of the IRAS 12 µm photometry, typically 6 to 9 percent. Photometry at other wavelengths was used only as a guide to the reasonableness of the final spectrum. This additional photometry was calibrated by a zero-order method that estimated spectral irradiances at the authors' reported effective wavelengths for their bandpass filters. In Version 2 we plan to normalize the spectra to all the "well characterized photometry" that is available for the star, using a technique similar to that used to produce the Walker-Cohen Atlas. That is, we will use all the photometry where the spectral

response of the system is known, its zero-point can be established on the common system defined by Cohen, et al. (1992), and the measurements are complete with uncertainties reported. Furthermore, in Version 2 we desire to make a more definitive treatment of the variability of the stellar spectrum than was done in Versions 1.0 and 1.1. To do this we require the dates of the observations. Therefore, we have compiled new expanded photometric databases from the available literature. Table 1 gives the status of the databases we have compiled to date. Compilation of new data continues to require most of our effort.

**Table 1. Current Database Status**

Catalog	IDL Code	No. of stars	No. of Observations	Original Units	Information Needed/Added
IRAS/WSDB	Read_iras.pro Star_colors.pro	1638	5287	Jansky	60 μm time-tagged WSDB
MSX	Read_Msx.pro	683		Jansky	Time-tagged data from Egan
SAAO	Read_Saao.pro	124	3553	Magnitude	
SMITH-DIRBE	Read_Dirbe.pro	38	Light curves in ≤ 6 bands	Jansky	
FOQUE	Read_Foque.pro	516 + 584	516+ 584	Magnitude	Calibration to be confirmed
JONES	Read_Jones.pro	13		Magnitude	
CIO	Read_Cio.pro	1693	29602	All units	Epochs, errors, response curves
2MASS		200 +	600 +	Jansky	Epochs
LRS		1638+ 664	8312 spectra	W/cm^2/μm	Time-tags, time-resolved spectra

3.2 Development of Model Spectra

In AFBSA Versions 1.0 and 1.1 the spectra were constructed from the LRS (for the mid-wavelengths) with the best-fitting spectra selected from the library of 87 SKY 4 categories (Cohen, et al., 1993) to extrapolate to longer and shorter wavelengths. During this process we noted that the grid of spectra available poorly fit many stars, and we concluded that a more extensive set of model spectra was in order.

We have adopted the DUSTY code (Ivezic, et al., 1997) since about 94 percent of the stars in the AFBSA V1.1 are AGB stars. DUSTY allows a wide range of input parameters to customize the models. Our plan is to compute two sets of grids, one for the oxygen-rich stars (AGBMs) and one for the carbon-rich stars (AGBCs). We have been exploring the range of model dust shell parameters, such as chemical composition, relative abundances, grain size distribution, dust density distribution, temperature at the inner dust shell boundary, and optical depth of the dust. The objective is to find those sets of parameters that produce spectra and colors that represent the stars in our list. Figures 1 and 2 show some of the model spectra produced. Each plot is for a fixed selection of all parameters except the optical depth (at 2μm), which is varied in 16 logarithmic steps from 0.001 to 10.

Figure 1 shows a set of models for a carbon-rich star with an abundance of 50 percent amorphous carbon and 50 percent silicon carbide grains. The grain size distribution is that given by Kim, Martin, and Hendry (1994) with the coefficients derived by Jura (1994) to well represent the dust distribution in IRC 10216. The temperature of the inner radius of the shell is 600K, and the density distribution is that determined by radiatively driven winds. The silicon carbide feature at 11μm is seen first growing in emission and then reversing to become an absorption feature as the optical depth increases.
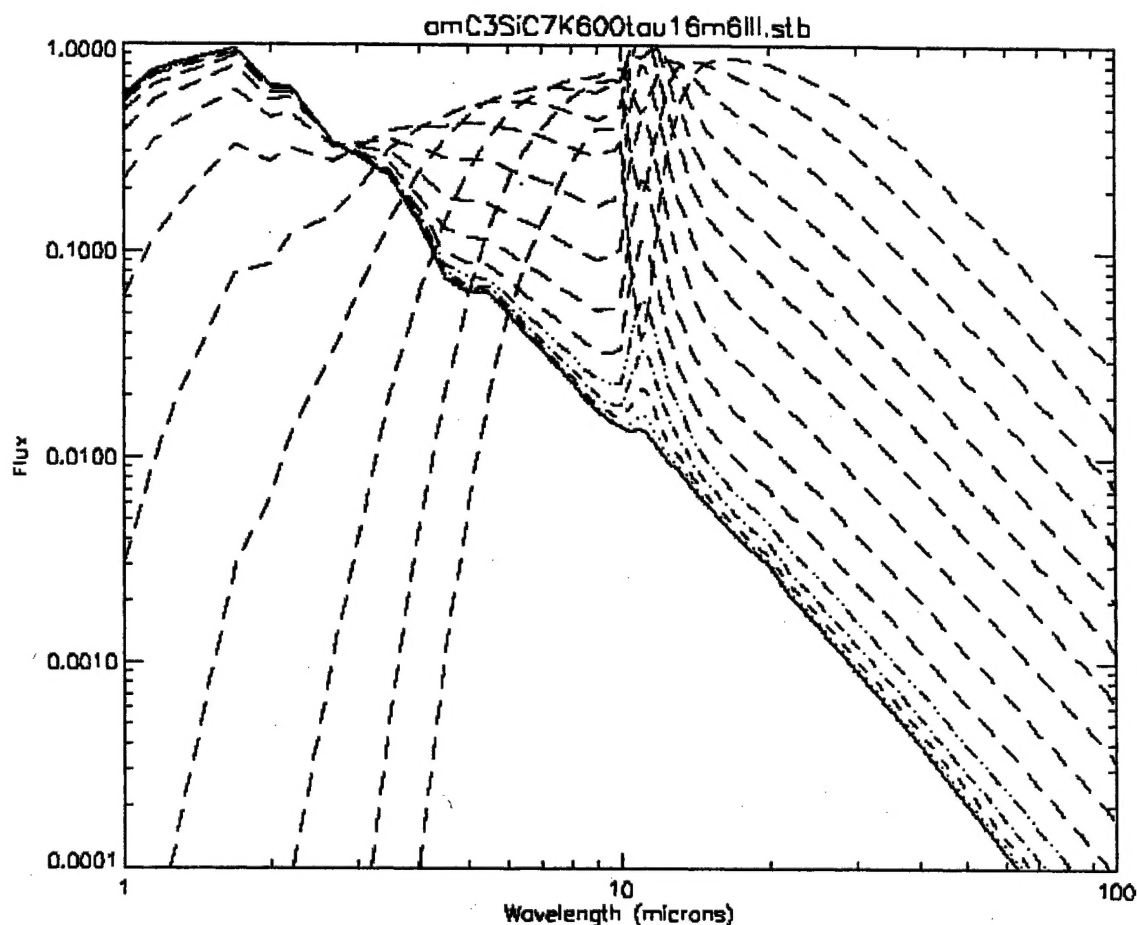

Figure 1. A Sample Of The DUSTY Models For Carbon-Rich AGB Stars. The Flux Given On The Ordinate Is The Spectral Flux λF_λ Normalized By The Integral Flux.

Figure 2 shows a set of models for an oxygen-rich star with inner shell radius at 500K, and grain size and density distributions as given above. The grain composition is that of warm astronomical silicates as given by Ossenkopff et al. (1992). The 10 and 20µm silicate features are easily seen, with the 10µm feature reversing from prominent emission to deep absorption as the optical depth is increased. It is clear in both figures that for even moderate optical depths the details of the input stellar spectrum are quickly lost and contribute little to the shape of the emergent dust spectrum.
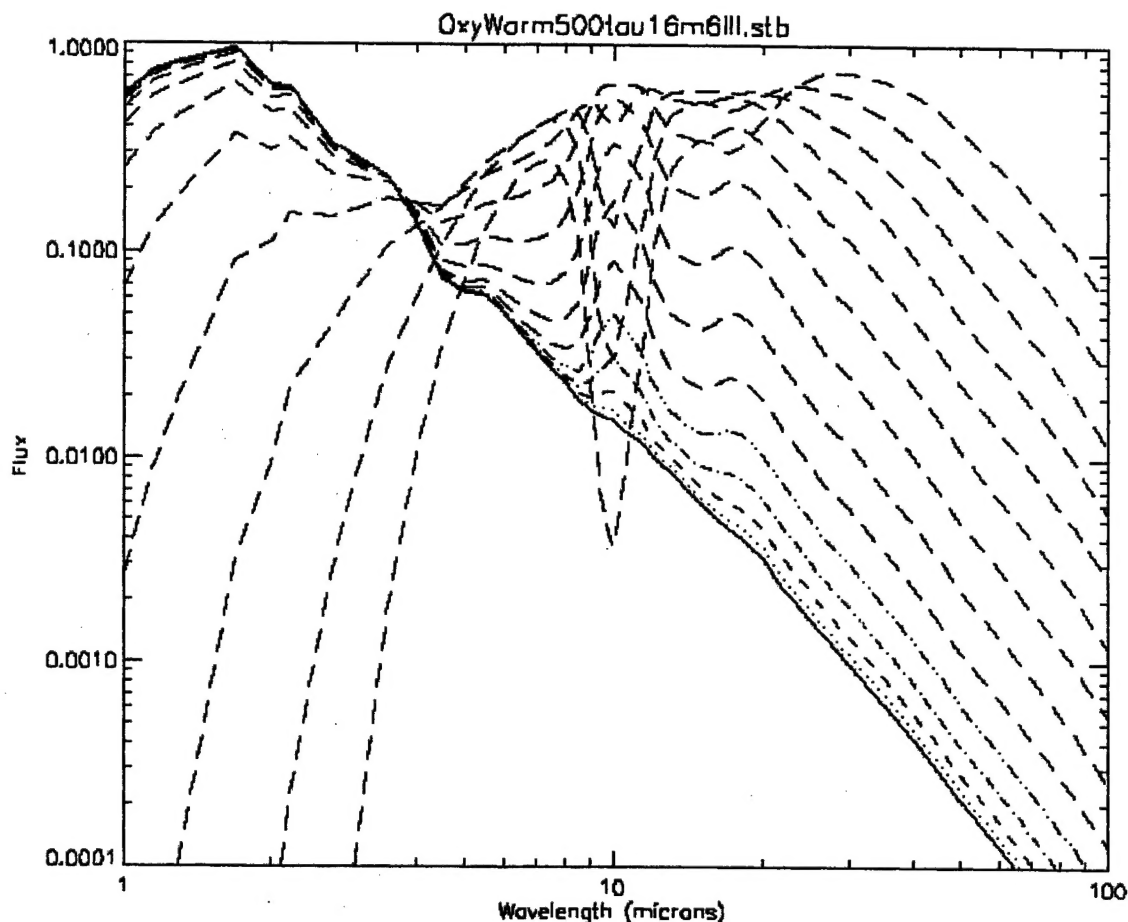
Figure 2. A Sample Of The DUSTY Models For Oxygen-Rich AGB Stars.

The production of Version 2.0 will use DUSTY model spectra selected from a sub-sample of the total DUSTY grid by their positions in the IRAS [12-25], [25-60] color-color plane. We will require that, although our final spectra extend out to only 30µm, the chosen DUSTY spectrum will be in agreement with the in-band fluxes observed by IRAS at 12, 25, and 60µm. Figure 3 is an example of how some DUSTY model IRAS colors extend through the region in the color-color plane. The boxes are the stellar occupation zones defined by Cohen and Walker (198x). It is clear that the requirement to reproduce the IRAS colors greatly constrains the range of applicable DUSTY spectra. It is also clear that a wider range of parameter space must be explored to produce models that will more densely populate the plane.
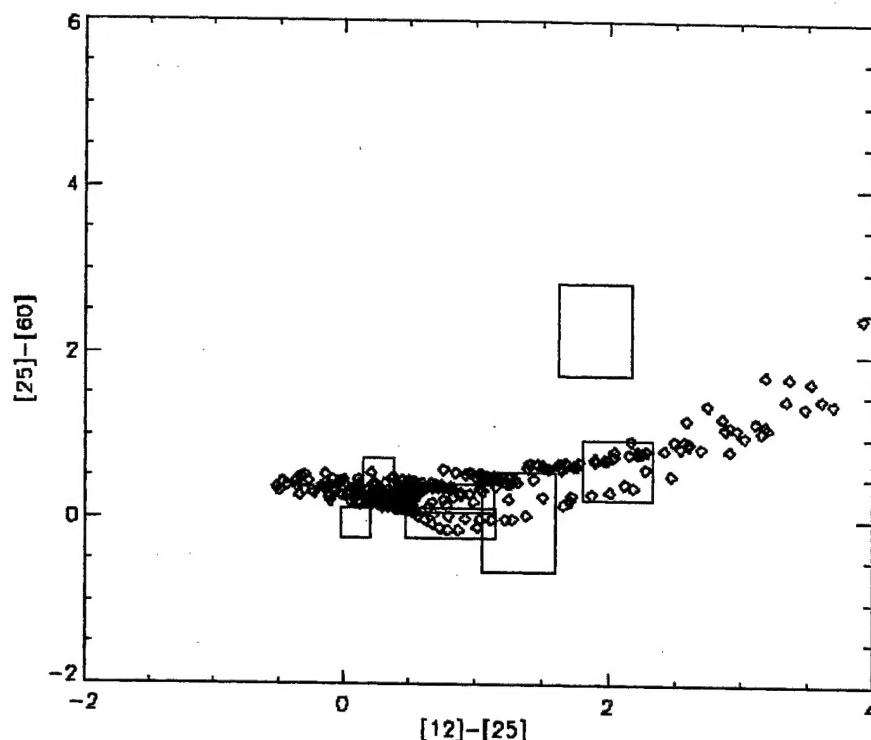
Figure 3. IRAS Colors Of Some DUSTY Models Superimposed On A Plot Of The Stellar Occupation Zones Of Cohen And Walker (198X).

4. NON-REJECTED LUNAR RADIANCE (NRLR)

The MSX/DCATT experiment DC32 was designed to characterize the SPIRIT III Out-of-Field-of-View-Rejection (OFVR) at off-axis angles within the SPIRIT III baffle cut-off by exploiting TDI and the multiband nature of the radiometer for measurements near the Moon. The Moon was used as the bright source of off-axis irradiance incident on the SPIRIT III telescope aperture. The SPIRIT III sensor scanned the radiance in a narrow 30°-long field with its long axis normal to the ecliptic plane and centered near a solar elongation of 180°. The apparent sidereal motion of the Moon varies with its position in its orbit over the range from 0.84 to 1.1 degrees per MSX orbit. Full moon occurs at the time the Moon is at a Sun-centered longitude of 180°. Therefore, in the case of 0.84°/orbit motion, 18 orbits prior to the orbit that can observe full moon the Moon is approximately 15.12° to the east of the field being scanned. On each subsequent orbit the Moon approaches the scanned field by an additional 0.84°. On the 19th orbit the scan passes over the Moon, and after another 18 orbits the Moon will be 15.12° west of the scanned field. In this way it was possible to map the OFVR of SPIRIT III in a 30° x 30° field centered on the Moon. The resolution of the map was approximately 0.84° in the Y coordinate and nearly single pixel resolution in the Z coordinate.

Scans that were made at the extremes of the field (± 15.12°) were to be used to determine the sky background in spatial regions that were near, but presumably, outside the SPIRIT III baffle cut-off and thus expected to be free of stray Lunar radiance. This natural sky radiance (zodiacal emission, stars, etc) must be subtracted from all of the scans in order to delineate that component of the total observed radiance due off-axis Lunar radiance. Subsequent analysis of

6

the SPIRIT III baffle indicated that the baffle angle was slightly greater than 16° and there was the real possibility that the extreme scans were contaminated by a small, but significant, amount of Lunar radiance. With this as a possibility, we were asked to develop another approach to extracting the Lunar OFVR from the DC32 observations, which did not rely on the "purity" of the extreme scans. The scheme that we developed is detailed in Appendix B.

5. NON-REJECTED EARTH RADIANCE (NRER) IN CB01

The MSX celestial experiment CB01 performed several long scans passing near the Sun to measure the infrared zodiacal radiance at small solar elongation angles. This was done during the time that the satellite was in the shadow of the Earth eclipsing the Sun. The scans thus passed close to the Earth's limb and non-rejected Earth radiance (NRER) contaminated the data. In fact, the NRER dominated the observed radiance over large portions of the scans and must be removed to recover the zodiacal radiance.

Independent measurements of the NRER were made in the DCATT experiment DC08 - SPIRIT III Earthlimb OFVR Characterization. In this series of experiments the SPIRIT III telescope was scanned into the Earth's limb and the resulting radiance profile recorded. This was done for a number of azimuth orientations of the MSX satellite and the resulting radiances mapped as a function of the tangent height of the line of sight and the azimuth rotation about the line of sight of the telescope. Each scan was made at a different time, when the satellite was passing over a different part of the Earth. This induced a third variable into the observed NRER, that due to the varying source (Earth) radiance which is dependent on the temperature, weather, cloud cover, etc. of the parts of the Earth that contribute to the NRER.

Previous reductions of the DC08 data did not attempt to account for the variations of the source of the NRER. This produced NRER curves at different azimuths that could not be related to one another due to source variations, and required special scaling to be applied. The approach explored here was to relate the various scans by normalizing them to a single source of radiance whose properties were determined by its color temperature. The in-band radiances measured at each tangent height for Bands A, C, D, and E were fit to a greybody spectrum, and the temperature of the best fit greybody determined. These are shown in Figure 4 where the color temperature is plotted versus tangent height for the DC08 scans. The temperatures deduced at tangent heights greater than 500 km are strongly effected by the SNRs and very sensitive to subtraction of the zodiacal background radiance, which was estimated from the observed radiance in the 700 to 800 km region. It is interesting to note that in the tangent height range from 200 to 450 km the deduced color temperature varies only a few degrees during a limb scan, while the non-rejected Earth radiance varies by an order of magnitude or more over the same range.

Our approach was to normalize all the scan radiances by the in-band blackbody radiance ratios of the radiance at the median temperature of the scans (determined in the 250 to 350 km region) to that of a blackbody at the observed color temperature. This would produce a new NRER matrix for a source at the median temperature. To apply this new matrix to observed data, one would measure the color temperature during the scan and correct the NRER matrix by the ratio of the radiances at the observed color temperature to that of the matrix temperature. At this point the work was terminated due to a different technique being pursued by AFRL. We believe that our approach has merit and intend to pursue it independently in the future.

7
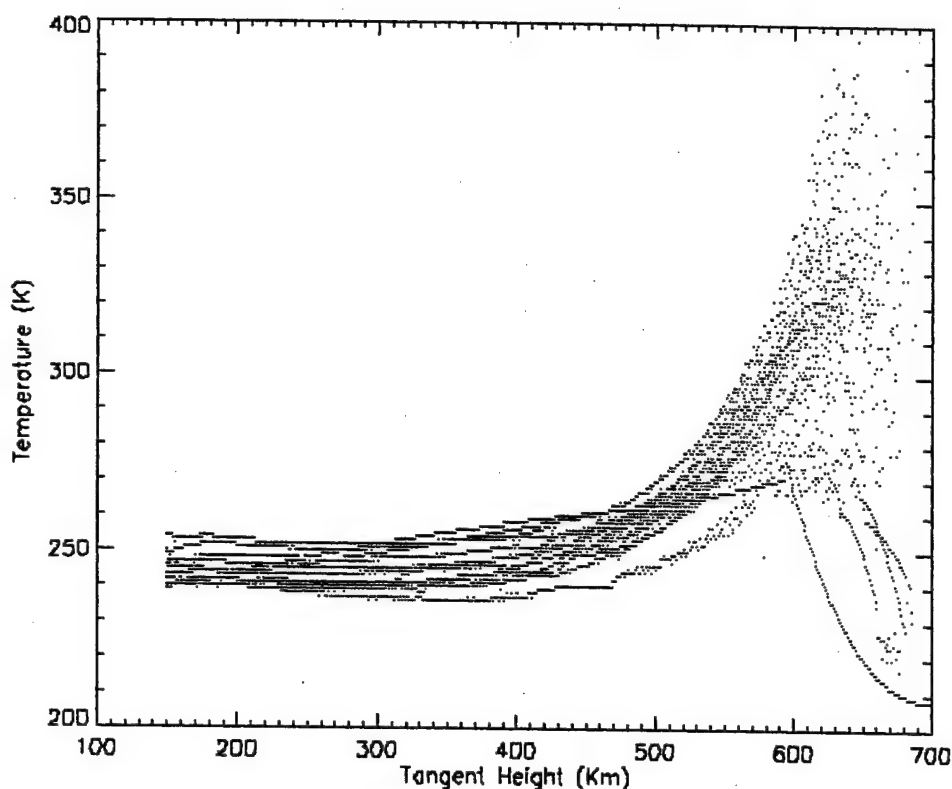
Figure 4. Color Temperature Plotted As A Function Of The Tangent Height Of The DC08 Limb Scans.

6. SOFTWARE DEVELOPED UNDER THE CONTRACT

The computer software identified in Table 2 and described in subsequent paragraphs has been developed, or is in the process of being developed in support of the contract goals.

6.1 Sky Model Extension

SKY5 is a program that statistically models the point source sky. It is an extension of SKY4 and adds the capability to handle user-supplied bandpass filters including narrow passbands. It consists of two FORTRAN codes, lum5.f (the executable) and special5.f (a version of lum5.f that runs in absence of a MONGO plotting package). Explain5.ps is a Postscript file explaining the new model and how to run it. It includes files of a new extinction law, newext.dat, and the hi-res Vega spectrum (vegahires.sky) that supports the user-supplied passbands. There is a new halo.dat look-up table for the galactic halo density, and the 87-category binary spectral library, library87.dat.

6.2 MSX Stellar Calibration Software

This is a suite of procedures to reduce MSX CB06 data, create images of the scans, photometer the individual scans, coadd the scans, and finally photometer the co-added images. All are written in Interactive Data Language (IDL). Cb06_final.pro reads the output data from the MAP files produced by CONVERT and POINTING CONVERT and creates an image for

8

Table 2. Software Developed Under Contract F19628-98-C-0047

TASK	SOFTWARE	STATUS
Sky Model Extension	SKY5: lum5.f, special5.f, vegahires.sky, halo.dat, library87.dat, newExt.dat, explain5.ps	Code delivered to AFRL on January 26, 2001 with documentation, installed, and tested on the AFRL computer Blaauw in the directory /home/celestial/cohen/sky5.
MSX Stellar Calibration	CB06: cb06_final.pro, photometer_cb06.pro, coadd_cb06.pro, column_background.pro, show_cb06.pro	Code and documentation was delivered to AFRL May, 2002 on CD ROMs which also contained the processed data.
MSX Zodiacal Radiance	CB-01: plot_zod_noNRER.pro read-dbfgen_nrer.pro DC-32: dc32_offset_onelong.pro	The software has not been delivered to AFRL. It is all quite specific to the MSX zodiacal radiance problem.
Lunar OFVR	DC-32: brdf.pro, curvefit_brdf.pro, dc32_moon.pro, dc32_scan.pro, noise_calc.pro noise_star_calc.pro, remove_stars.pro, moonflux.for, moonscan.for	Not delivered. The project was terminated prior to completion. Much of the software is in a state of partial development. Little documentation exists.
AFBSA	afbsc.pro, afbsc11.pro, calibrate_afgl.pro, cio_flux_cal.pro, cal_factor.pro, and a large suite of utilities	This software has not been delivered to AFRL. It is all quite specific to the production of the various versions of the AFBSA. Much of this is being modified and incorporated into code being developed for Version 2 of the AFBSA.

each detector column for each scan in the CB06. Photometer_cb06.pro locates the standard star in the image, creates a mini-image of the region containing the star, and performs aperture photometry of the star. Coadd_cb06.pro spatially coadds the mini-images of the stars. Provision is made for a "blind" coadd using all images, or a selective coadd from viewing the image sets. Column_background.pro and show_cb06.pro are CB06 utilities.

6.3 MSX Zodiacal Radiance

A set of two programs written in IDL form the code for the analysis of the CB01 data that was delivered by AFRL. Plot_zod_noNrer.pro is a first order of removal of the NRER from the CB01 scans to extract the zodiacal radiance. The program assumes the zodiacal cloud to be symmetric about the location of peak radiance and determines the extent of the NRER contamination. The NRER values are compared to the empirical NRER model and the scaling factor to correct the difference between the model and the data are determined for each waveband.

The Read_dbfgen.pro reads in the data, that inputs the total radiance measurements as a function of ecliptic latitude and longitude. It has two versions, the later version was modified to read the newer data set which included the tangent height as well as the roll angle values. The code estimates the NRER values using the tangent height and roll angle.

Dc32_offset.pro uses a list of subroutines that is part of the Lunar OFVR calculation in order to create a scan from the output of Pointing Convert data. The code removes the data that does not have offset measurements, limits tangent height to remove NRER contamination and also removes stellar point sources. The final scan of radiance as a function of ecliptic latitude shows the zodiacal component in the DC32 data.

6.4 Lunar OFVR

This is a set of programs and procedures to attempt to re-evaluate the out-of field-of view-rejection (OFVR) of the MSX SPIRIT III telescope. Brdf.pro is a procedure to estimate the BRDF of the SPIRIT III telescope mirror from the DC32 near Lunar scans. Curvefit_brdf.pro is a modified version of the IDL curvefit routine that performs a non-linear least squares fit to a function of an arbitrary number of parameters. DC32_moon.pro reads the output data from POINTING CONVERT MAP file and creates a fits image for each scan near the Moon. Dc32_scan.pro, noise_calc.pro, noise_star_calc.pro, and remove_stars.pro are utilities to support the main program. These are all coded in IDL.

Moonflux.for and moonscan.for are FORTRAN programs to calculate the irradiance of the moon in the SPIRIT III bands.

6.5 AFBSA

These are computer programs that are used to assemble and produce the Air Force Bright Spectral Atlas (AFBSA), Versions 1.0, 1.1, which have been published, and Version 2.0 which is currently being worked on. Afbsc.pro and afbsc11.pro are the production programs for Versions 1.0 and 1.1. These are procedures to classify an IRAS LRS spectrum by fitting to one of the Sky Templates, attach photometry, and output an AFBSC_ver_1.x spectrum. Calibrate_afgl.pro, cio_flux_cal.pro, and cal_factor.pro are used to calibrate the major uncalibrated input data files. There are also numerous utilities, written both in IDL and FORTRAN, that are used to search data bases, extract necessary information about the star observations, and format those data as to be useable by the atlas production programs.

REFERENCES

Cohen, M., Walker, R.G., Barlow. M.J., and Deacon, J.R., 1992, Spectral Irradiance Calibration in the Infrared, I. Groundbased and IRAS Broadband Calibrations, *Astron. J.* Vol **104**, No.4, 1650-1657.

Cohen, M., Walker, R.G. and Witteborn, F.,1992, Spectral Irradiance Calibration in the Infrared, II. Alpha Tau and the Recalibration of the IRAS Low Resolution Spectrometer, *Astron. J.* Vol **104**, No.5, 2030-2044.

Cohen, M., Witteborn, F.C., Carbon, D.F., Augason, G.C., Wooden, D., Bregman, J.D., & Goorvitch, D. 1992, Spectral Irradiance Calibration in the Infrared, III. The Influence of CO and SiO , *Astron. J.*, **v104**, 2045

Cohen, M., Witteborn, F.C., Walker, R.G., Bregman, J.D., and Woden, D.H., 1995, Spectral Irradiance Calibration in the Infrared, IV. 1.2-35 Micron Spectra of Six Standard Stars, *Astron. J.* , vol. **110**, no. 1

Cohen, M. & Davies, J.K. 1995, Spectral Irradiance Calibration in the Infrared, V. The Role of the UKIRT and the CGS3 Spectrometer, *Mon. Not. Roy. Astron. Soc.*, **v275**, p715

Cohen, M., Witteborn, F.C., Bregman, J.D., Wooden, D.H., Salama, A., & Metcalfe, L. 1996, Spectral Irradiance Calibration in the Infrared, VI. Three Southern Standards, *Astron. J.*, **v112**, p241

Cohen, M., Witteborn, F.C., Carbon, D.F., Davies, J.K., Wooden, D.H., & Bregman, J.D. 1996, Spectral Irradiance Calibration in the Infrared, VII. New Composite Spectra, Comparisons with Model Atmospheres, and Far-IR Extrapolations, *Astron. J.*, **v112**, p2274

Cohen, M., Witteborn, F.C., Roush, T., Bregman, J.D. & Wooden, D.H. 1998, Spectral Irradiance Calibration in the Infrared, VIII. 5-14 Micron Spectroscopy of the Asteroids Ceres, Vesta, and Pallas, *Astron. J.*, **v115**, p1671

Cohen, M., 1998, Spectral Irradiance Calibration in the Infrared, IX., Calibrated Stellar Spectra Using DIRBE Radiometry, *Astron. J.*, **v115**, p2092

Cohen, M., Walker, RG, Carter, B., Hammersley, P., Kidger, M. and Noguchi, K., 1999, Spectral Irradiance Calibration in the Infrared. X. A Self-Consistent Radiometric All-Sky Network of Absolutely Calibrated Stellar Spectra, *Astron. J.*, **117**, 1864-1889

M. Cohen, 1993, A Model for the 2-35 micron Point Source Infrared Sky, *Astron. J., **105**, 1860*

Ivezic, v Z. & Elitzur, M. 1997, Self-similarity and Scaling Behavior of Infrared Emission from Radiatively Heated Dust, I. Theory, *Mon. Not. Royal Astron. Soc.* **287**, 799; Erratum:1999, *Mon. Not. Royal Astron. Soc.* **303**, 864

Jura, M. 1994, The Particle-Size Distribution In The Dust Ejected From IRC +10216, *Astrophys. J.*, **434**, 713

Kim S.H., Martin P.G. & Hendry P.D. 1994, The Size Distribution Of Interstellar Dust Particles As Determined From Extinction, *Astrophys. J.*, **422**,164

Mathis J.S., Rumpl W. & Nordsieck K.H. 1977, The Size Distribution Of Interstellar Grains, *Astrophys. J.*, **217**, 425

Ossenkopf, V., Henning, Th. & Mathis, J.S. 1992, Constraints On Cosmic Silicates, *Astronomy & Astrophysics*, **261**, 567

Appendix A. Walker-Cohen Atlas Of Calibrated Spectra - Explanatory Supplement

1. Introduction

The 603 templates issued under Release 4.0 were formulated following essentially the same principles as in previous releases (Release 2.1 Cohen et al. 1999; Release 3.0 April 2001). However, to make sure that templates (1.2-35 micron spectra) and our new "supertemplates" (0.11-35 micron templates) to be constructed for use by SIRTF's instruments are not represented by different spectral energy distributions where they overlap, several changes were made to the template code at this time. This document describes these changes and their implementation in Release 4.0.

Much of the text below duplicates the documentation accompanying Release 3.0 and has been retained for completeness between the published Release 2.1, and the new Release 4.0 network of stellar calibrators. However, wherever further changes have occurred between Releases 3.0 and 4.0, these are described in the appropriate sections.

2. New Composites and Stars to Template

2.1. Walker-Cohen Atlas: K4IIIs

Of the original 573 stars in the Walker-Cohen Atlas (Walker & Cohen 1992: WCA), we templated 422 in 1998-99. The largest gap in our list of "templatable types" was represented by K4III due to our inability to couple KAO 5-8 micron spectra of β UMi with any ground-based 1-5 micron spectral data (the star is simply too far north to be observed by the relevant telescopes that had good IR spectrometers available). This omission cost a total of 56 stars of type K4III (we handled K3.5IIIs using our K3III, and K4.5IIIs using our K5III template).

Therefore, we deemed it prudent to create a K4III "template" by interpolation between the smoothed K3 and K5 templates. To achieve this, we first separated the global and local biases from the purely uncorrelated uncertainties in the two flanking template spectra, and linearly interpolated between the random variances associated with the K3 and K5 spectra. Interpolation was linear, but in the quantity "s", described by de Jager & Nieuwenhuijzen (1987), and demonstrated to be a far more linear mapping of spectral type than any quantity such as (B-V) or effective temperature. Local and global biases were interpolated by the identical method, then the three components of total error were reassembled for the final K4III template. Note also that this approach gave us the opportunity to regrid the K3III template (from α Hya in whose commmposite spectrum there still lingers a gap from 2.4 to 2.9 microns, never covered adequately with the existing KAO data) onto the continuous α Tau K5III spectrum, thereby eliminating this gap from the newly-built K4III spectrum.

However, as an end-to-end check of the reasonableness of the derived spectrum, we compared the K4 template with the shape of the β UMi KAO 5-8 micron spectrum, spliced to the 7.7-22.7 micron LRS spectrum. The agreement was satisfactory (i.e. within the observational

uncertainties in the airborne and IRAS data), and we deemed it appropriate to proceed with this K4 "composite".

All that was then required, to apply the K4III template exactly as its forerunners, was an angular diameter calibrator. For this we used two stars for robustness: β UMi and β Cnc. The former is the brighter of the two yet its angular diameter is the more poorly measured: Dyck, van Belle & Thompson (1998) give 9.7+/-0.8 milliarcsec, compared with β Cet measured by Nordgren et al. (1999) who give 5.03+/-0.04 milliarcsec). Both diameters were used to template β UMi itself with the K4III construct. The observed diameter for β UMi was used to fix the correct fractional uncertainty while β Cnc's observed diameter determined the correct angular diameter scale.

2.2 ISO Calibrators

Following the demonstrated success of ISO's calibration, and our paper showing that MSX and ISO are equivalent radiometrically in terms of the observed MSX irradiances of over 100 stars that were originally selected to support ISO's potential need for a network of absolute calibrators (Cohen, Hammersley & Egan 2000), we tackled 46 stars of the ISO "Ground-Based Preparatory Programme" that were templatable, cool giant stars but were erroneously represented for ISO purposes by Kurucz models. All these Kurucz "calibration spectra", of course, lacked the SiO fundamental and were based on outdated CO line strengths. Consequently, our goal was to reissue their spectra as CWW templates, appropriate to their types. These stars are, therefore, included in Release 4.0 and often are significantly fainter than the IRAS 12-micron flux density limit of 5 Jy that characterized our earlier releases.

2.3 MIRS Calibrators

In the intervening 3.5 years since Release 2.1 templates were first created, we have received requests from the Japanese for help in calibrating their Mid-Infrared Spectrometer on the joint NASA-ISAS "Infrared Telescope in Space" mission. This mission covered 7% of the sky and the need was to provide as many absolute calibrators as possible in that fraction of the sky. The brightest stars well-detected by MIRS (a 32-element array of detectors covering 4.6-11.6 microns continuously) were extracted and their names provided to us. We selected a number of stars for which it seemed we might be able to offer templates if we could significantly extend our range to M4III.

Consequently, founded upon our gamma Crucis composite (M3.4III), we extended to templates as late as M4III. Some of the stars selected for MIRS were wildly variable. These objects were never used for MIRS calibrators and were never issued as calibrated templates in Release 3.0. However, 19 stars became valuable MIRS calibrators and, therefore, also appear among the new templates of Release 4.0.

To satisfy the need to handle any M-giant from M0-M4, we also used the α Cet (M1.5III) composite to create another smoothed template, filling in from M1-M1.5III, while β Peg (M2.5II-III) serves to template M2-M3 stars, and γ Cru is applied solely to M3.5-4III types.

2.4 The New γ Cru Composite (M3.4III)

The latest stars of the network are provided by the template derived from the composite spectrum for γ Cru. When the γ Cru composite was built (in 1996), the available photometry for this star was woefully sparse and poorly traceable to any modern, quantitative context. However, following the "CB-06" experiment on MSX, good traceable radiometry of this star was secured. As a consequence, it has become possible to construct a more reliable composite. Further, the 1996 γ Cru was extended down to 1.2 microns (from the original shortest KAO-observed wavelength of 3.95 microns) in order to take advantage of template stars with characterized short-wavelength photometry. At the time, the extrapolation was performed using a model atmospheric spectrum due to Kurucz (1994) to extend below the initial observed wavelength of 3.95 microns. The current public availability over the Web of the NextGen Giant grid of stellar model atmospheres and synthetic spectra (Hauschildt et al. 1999) makes it possible now to further upgrade to a state-of-the art model with a correspondingly more realistic synthetic spectrum. This we have done, merging the NextGen spectrum with our old empirical γ Cru spectrum at 9.8 microns. Below this wavelength we adopted the NextGen spectrum; above, we took our original composite. There is excellent accord between the two beyond this wavelength. Indeed, we can now appreciate that the pristine KAO-LRS splice from 7.5 to 9.3 microns was flawed by poor LRS data, leading to a spectrum below about 7.0 microns at a flux density level too high compared with that longward of 9.8 microns.

We have tested the newly adopted composite/template for γ Cru against this star's MSX CB06 photometry and have achieved a most satisfactory match. In fact, we have also been able to improve our Release 2.1 estimate for the angular diameter of γ Cru from 26.06 to 25.35 mas. This new value is afforded by the Release 4.0 template for the M4III ρ Per (HD 19058), for which di Benedetto & Rabbia (1987) published a limb-brightened angular diameter of 15.5 mas, which we have used to renormalize γ Cru's diameter. Using the new γ Cru template we achieved excellent accord with all the M3.5 and M4IIIs in the network; i.e. the reddened templates provide very good matches to all the photometric points available for our subset of 1 M3.5III, 4 M3/4IIIs, and 15 M4IIIs.

2.4 DIRBE "BCC" Calibrators

We have further exercised DIRBE's own calibration network, whenever those stars have templatable types (we abandoned all stars later than M4III), drawing from the 92 objects in the "BCC" archive discussed by Mitchell et al. (1996). This is permitted because we have already demonstrated (Paper IX) that DIRBE faithfully replicates our calibration context. The templates for the latest type BCC calibrators are now also improved in Release 4.0, for the reasons just described.

3. New Photometry Resources

3.1 The Literature & the ISO GBPP

To provide normalizations for all these additional templates we found a handful of additional photometry archives in the published literature that were traceable as to passband, uncertainties,

and zero points (e.g. Kerschbaum & Hron 1994; Kerschbaum et al. 1996). A new major resource came about because of the public release of even more ISO data through their "Ground Based Preparatory Programme" (GBPP) of supporting photometry, primarily from Hammersley, both broadband (JHK) and narrowband Selby-type (Jn,Kn, Ln). These sufficed to normalize the many ISO Hipparcos-selected cool giants.

3.2 MSX

Following our paper based on the CB06 DCEs (Cohen et al. 2001), we have now incorporated the ability to use either MSX PSC1.2 or CB06 data in template normalization.

3.3 DIRBE "BCC" Data

We are content to utilize DIRBE photometry for BCC stars, but only after proper allowance for the uncertainties that arise in each band as a consequence of the uncertainties in solid angle for each of bands D1-D4, and for the Poisson fluctuations in the background around each star to be templated, in addition to the regular statistical errors derived from the very large number of measurements per band per star.

3.4 η Sgr - A Special Case

In the early days of infrared photometry, the bright M2II star, η Sgr, was a popular calibrator. We notice a tendency for the newest observations on Keck and/or Gemini telescopes, for example with the OSCIR instrument, to return to use of this star. We have, therefore, decided to create a CWW style template for this star based on published South African near-infrared magnitudes, and mid-infrared magnitudes directly against Sirius by Cohen & Barlow (1980).

3.5 The Role of IRAS

In previous releases of templates, we could count on the existence of 4 meaningful PSC/FSC flux densities at 12/25 microns for each star. However, with the increased diversity of stars now, and the associated faintness of some objects, this is no longer the case. We have modified the template code to be capable of addressing a wide variety of less than ideal but real-life situations, such as no PSC data yet FSC are present; no 25-micron flux densities, only those at 12 microns, be they PSC or FSC; etc.

4. New Spectral Types

The release of the Fifth Volume of Michigan Spectral Types (Houk & Swift 1999) has had a major impact on our templates. Finally, this single-person consistent effort at spectral classifications has crossed the celestial equator, necessitating a reevaluation of all the types on which we base our choice of template. Our choice in 2002, is as in 1999, 1. Michigan; 2. Perkins Revised; 3., and a poor choice even for third place, the BSC version 5 (whose rich detail of declared types obscures the fundamental heterogeneity and incorrectness of many). Consequently, we designed the choices for all 690 stars available to us for the new release to follow this rigid prioritization. Thus, even if some stars have only the same photometry as was

available to us for Release 2.1, they could still be represented in Release 4.0 by a different template because their spectral types may have been reclassified by the Michigan project in the intervening years.

5. Extinction

Since Release 3.0 we have reevaluated the intrinsic B-V color tables for templatable K- amd M-giants on the basis of substantial samples of these stars that were observed by Hipparcos. Utilizing solely those cool giants with significant (typically >5 sigma) parallaxes, we have determined the absolute B and V magnitudes of samples with some tens to hundreds in each spectral subclass. These have also been tested in our experiments to predict near-IR magnitudes (JHK) for potential SIRTF calibrators working solely from spectral type and precision optical photometry. The resulting set of newly defined intrinsic B-V colors is now incorporated into Release 4.0.

As in previous template networks, our preference is to use published estimates of E(B-V) or Av for the K- and M-giants in our sample. We have enlarged the set of giants in this category based on the complete tables of extinction (or color excess) published either by McWilliam (1990) or Feast, Whitelock & Carter (1990) for cool giants. When these are unavailable we use E(B-V) and a total-to-selective extinction ratio of 3.10 (Barlow & Cohen 1975).

In previous releases we chose to set the extinction to zero for those stars in which the application of the reddening (Av<=0.044) would result in less than a 1% change in the monochromatic flux density at a wavelength of 1 micron. However, for Release 4.0 we always applied the reddening regardless of the size of its effect in the near-infrared to avoid potential discrepancies between templates created by our conventional (1.2-35 micron) technique and supertemplates (0.11-35 micron spectra) created for SIRTF and other missions, because supertemplates are always based on optical photometry and spectra where the reddening corrections are important no matter how small at 1 micron.

6. Templates

Templates are fashioned virtually exactly as before in terms of their header information. After their final creation, all 603 spectra were inspected to determine how well they fit their photometry, to check for erroneous photometry and/or uncertainties, and for correct transfer of names, etc. We visually examined our associated plots of these products to cull inappropriate data. All 603 passed inspection.

7. An Overview

7.1 Template Types
The breakdown by giant template types is as follows: 82 β Gem (G9.5-K0.5); 106 α Boo (K1-2); 96 α Hya (K2.5-3.5); 76 β UMi (K3.5-4); 121 α Tau (K5-7); 68 β And (K8-M0.5); 10 α Cet (M1-1.5); 24 β Peg (M2-3); 20 γ Cru (M3.4-4).

7.2 Template Extinctions

396 of the 603 stars suffer zero extinction; the remaining 207 stars have extinctions between 0.02 and 1.77 mag, with only 33 values exceeding 0.50 mag.

7.3 Normalization Biases

Template normalization biases vary from 0.44% to 5.30%. Of these, 236 have bias <=1%, 424 <=2%, 525 <=3%, and 551 <=4.0%. Above 4%, biases usually correspond to normalizations based on IRAS data only.

7.4 Angular Diameters

Radiometric angular diameters range from 0.33 to 15.49 milliarcsec.

7.5 The Amount of Photometry per Template

The minimum number of pieces of normalizing photometry was 3; the maximum, 25. With 4 pieces there are 51 templates; with 5, 106; 6, 41; 7, 77; 8, 80; 9, 37; 10, 41; 11, 41; 12, 30; 13, 3; 14, 20; 15, 13; 16, 10; 17, 8; 18, 9; 19, 8; 20, 3; 21, 5; 22, 2; 23, 6; and 25 with 1.

8. References

Barlow, M.J. & Cohen, M., 1977, *Astrophys. J*, **213**, 737.

Cohen, M. & Barlow, M.J., 1980, *Astrophys. J*, **238**, 585.

Cohen, M., Hammersley, P.L., & Egan, M.P., 2000, *Astron. J*, **120**, 3362.

Cohen, M., Walker, R. G., Carter, B., Hammersley, P. L., Kidger, M. R., & Noguchi, K., 1999, *Astron. J.*, **117**, 1864.

Cohen, M., Walker, R.G., Jayaraman, S., Barker, E., & Price, S.D., 2001, *Astron. J.*, **121**, 1180.

de Jager, C. & Nieuwenhuijzen, H., 1987, *Astron. & Astrophys.*, 177, 217.

di Benedetto, G. P. & Rabbia, Y. ,1987, *Astron. & Astrophys.*, **188**, 114.

Dyck, H.M., van Belle, G.T., & Thompson, R.R., 1998, *Astron. J.*, **116**, 981.

Feast, M., Whitelock, P.A., & Carter, B., 1990, *Mon. Not. Royal Astron. Soc.*, **247**, 227.

Hauschildt, P. et al., 1999, *Astrophys. J.*, **525**, 871.

Houk, N. & Swift, C., 1999, ``Michigan Catalogue Of Two-Dimensional Spectral Types For The HD Stars, Vol. 5" (Ann Arbor, Michigan : Department of Astronomy, University of Michigan) .

Kerschbaum, F. & Hron, J., 1994, *Astron. & Astrophys.*, **106**, 397.

Kerschbaum, F. et al., 1996, *Astron. & Astrophys.*, **118**, 397.

McWilliams, A. 1990, ApJS, 74, 1075.
Mitchell, K. J. et al., 1996, in ``Unveiling the Cosmic Background", ed. E. Dwek, AIP Conf. Ser. 348, pg.301.

Nordgren, T.E. et al., 1999, *Astron. J.*, **118**, 3032.

Walker, R. G. & Cohen, M., 1992, "An Atlas of Selected Calibrated Stellar Spectra", NASA Contractor's Report CR-177604 to NASA Ames.

Appendix B. Derivation of SPIRIT III PSRR

In the DCATT experiment, DC32 scans of SPIRIT III were made at varying angles from the Moon. The radiance, R_{OBS}, that is observed by a single pixel in the focal plane is the sum

$$R_{OBS} = R_B + R_{NRLR} + R_{NRER} + R_{DO} \qquad (1)$$

Where R_B is the radiance from the sky background, R_{NRLR} is the out-of-field radiance from the Moon, R_{NRER} is the out-of field radiance from the Earth, and R_{DO} is the equivalent dark offset radiance.

It is our desire to isolate R_{NRLR} and from it deduce the PSRR of SPIRIT III and perhaps some of the pertinent telescope parameters. To accomplish this we will assume that the dark offset has been well modeled by the PL process and thus $R_{DO} = 0.0$. We will also reduce R_{NRER} to zero by using only fluxes that were observed at tangent heights greater than 650 km, where the NRER is negligible.

R_B is composed of the radiance of the zodiacal background + unresolved faint stars + resolved bright stars. We will reduce the effects of bright stars (and glitches) by thresholding the single pixel data stream according to Bloom's theory of ordered statistics applied to that local data block (71 samples). Samples that exceed the threshold will not be used in the "binning" process (see below). Using only observations that are well off the galactic plane could minimize the effects of unresolved stars. This, however is not possible for the set of observations DC32...12 through DC32...18. We will estimate the contribution to the background due to the unresolved stars using the LUM module of SKY5. At this point we assume that $R_B = R_Z + R_{LUM}$. The zodiacal radiance, R_Z, is a function of the solar elongation, latitude, and time of the observation. We will interpolate the grid of CB04 observations to the coordinates of DC32 observation. We will adopt this as representative of the zodiacal radiance in the DC32 DCE to within a scale factor, A_Z, (of order unity) to account for the variation due to observations at different times of the year. R_{LUM} is a function only of the galactic coordinates of the observation and the threshold flux for bright star removal. Note that each scan of the 7 DCE set repeats the same range of ecliptic latitude and longitude, and thus the same range of galactic coordinates as well. We are in the process of calculating $R_{LUM}(\theta)$ and will assess the importance of this term in the solution.

The non-rejected Lunar radiance, R_{NRLR}, is modeled as the sum of the radiance scattered by the primary mirror, R_{BRDF}, the radiance diffracted by the primary mirror, R_{DIF}, and higher order terms, R_{2nd}. The mirror scatter term is

$$R_{BRDF} = BRDF(\theta)\ V(\theta,\varphi)\ F_{moon}\ \cos(\theta) \qquad (2)$$

The bi-directional reflectance distribution function is modeled by

$$BRDF(\theta) = BRDF(1^\circ)\ \theta^{-n} = A_{BRDF}\ \theta^{-n} \qquad (3)$$

and

$$\pi V(\theta,\varphi) = 2 \cos^{-1}[\tan^{-1}(\varphi)\tan(\theta)] - \sin\{2 \cos^{-1}[\tan^{-1}(\varphi)\tan(\theta)]\} \qquad (4)$$

where θ is the off-axis angle to the Moon and φ is the limiting baffle angle which is $16.6°$ in the SPIRIT III X-Y plane and $18.1°$ in the X-Z plane. Thus φ is a function of θ and the closest approach of the scan to the moon, θ_{MIN}. We will attempt to correct for the "elliptical" shape of the limiting baffle angle by the following equation for the ellipse

$$\varphi^2 = a^2 b^2 (a^2 \sin^2 \alpha + b^2 \cos^2 \alpha)^{-1} \quad \text{and} \quad \sin \alpha = \theta/\theta_{MIN} \qquad (5)$$

where $a = 16.6$ and $b = 18.1$.

The diffraction term can be approximated (Dowling, private communication) by

$$R_{DIF} = A_{DIF}\, \lambda\, \theta^{-3}\, F_{moon} \qquad (6)$$

where λ is the effective wavelength of the response in microns. The higher order terms are also given by Dowling as

$$R_{2nd} = A_{2nd}\, \theta^{-0.5}\, F_{moon} \cos \theta \qquad (7)$$

Combining the above terms we may write

$$R_{OBS}(\theta) = A_Z R_Z(\theta) + R_{LUM}(\theta) + A_{BRDF}V(\theta,\varphi)\theta^{-n} F_{moon} \cos(\theta)$$
$$+ A_{DIF}\lambda\theta^{-3} F_{moon} + A_{2nd}\theta^{-0.5} F_{moon} \cos(\theta) \qquad (8)$$

Dividing by the Lunar flux, substituting $A_{DIF,\lambda} = A_{DIF}\lambda$ and $A_{Z,F} = A_Z/F_{moon}$, and rearranging equation 8 becomes

$$[R_{OBS}(\theta) - R_{LUM}(\theta)]/F_{moon} = A_{Z,F}\, R_Z(\theta) + A_{BRDF}V(\theta,\varphi)\theta^{-n} \cos(\theta) + A_{DIF,\lambda}\, \theta^{-3}$$
$$+ A_{2nd}\, \theta^{-0.5} \cos \theta \qquad (9)$$

We will solve for the n and A coefficients and their uncertainties using an IDL function CURVFIT that uses a gradient-expansion algorithm to compute a non-linear least squares fit of equation 9 to the observations. It is possible to develop a solution for each DCE separately or a global solution that uses the data from all 7 DCEs. We will pursue both solutions. Each spectral band is considered separately, however, we expect that the diffraction coefficient, $A_{DIF,\lambda}$, will be a linear function of the wavelength.

F_{moon} is calculated from a simple model of the Lunar surface radiance and is constant during each scan (to the fourth significant figure).

$R_{OBS}(\theta)$ is obtained by binning each pixel response into $0.1°$ bins of $R_{OBS}(\theta)$. CONVERT and POINTING are run on the data from each DCE and MAP files created. These are files of time and position tagged pixel responses. θ is calculated from the time and position, and the inverse variance weighted pixel response summed into the appropriate angle-from-the-moon bin.

The inverse variance is also summed into $1/\sigma^2(\theta)$ bins. The solar elongation and ecliptic latitude are also calculated for that sample and the zodiacal radiance interpolated from the CB04 grid. The zodiacal radiance is then summed into a $R_Z(\theta)$ bin. The galactic coordinates are calculated and the galactic unresolved-star radiance interpolated in the grid previously calculated by LUM. These are summed into $R_{LUM}(\theta)$ bins. In terms of the binned data the Rs of equation 9 are replaced by:

$$R_{OBS}(\theta) = \Sigma\ w_i\ R_{OBS,i}(\theta)\ /\ \Sigma\ w_i\ , \quad \text{where } w_i = 1/\sigma_i^2 \text{ and } \sigma_i \text{ is the noise of a single pixel,}$$

$$R_{LUM}(\theta) = 1/N\ \Sigma\ R_{LUM,i}(\theta)\ \text{ and }\ R_Z(\theta) = 1/N\ \Sigma\ R_{Z,i}(\theta)\ \text{ and N is the number of samples.}$$

prior to solving for the constants.

Partial Derivatives for CURVFIT

Make the following substitutions:

$$Y = [R_{OBS}(\theta)\text{-}R_{LUM}(\theta)]/F_{moon}\ ,\ a = A_{Z,F}\ ,\ b = A_{BRDF}\ ,\ c = A_{DIF,\lambda}\ ,\ d = A_{2nd}\ ,\ e = n$$

Then equation (9) becomes

$$Y = a\ R_Z(\theta) + b\ V(\theta,\varphi)\theta^{-e}\cos(\theta) + c\ \theta^{-3} + d\ \theta^{-0.5}\cos\theta$$

The partials with respect to the constants are then

$$dY/da = R_Z(\theta)$$

$$dY/db = V(\theta,\varphi)\theta^{-e}\cos(\theta)$$

$$dY/dc = \theta^{-3}$$

$$dY/dd = \theta^{-1/2}\cos\theta$$

$$dY/de = b\ V(\theta,\varphi)\theta^{-e}\ln\theta$$